

This work was carried out in the Department of Chemical Technology, Imperial College, London as part of the research programme of the Joint Fire Research Organization of the Department of Scientific and Industrial Research and Fire Offices' Committee. The authors are indebted to the Director for permission to publish this account.

The authors are also indebted to Dr C. S. Chow, of this Department, for measurements of the purity of the gases employed and for the detailed analysis of the sample of coal gas.

REFERENCES

- Coward, H. F. 1919 *J. Chem. Soc.* **115**, 27.
 Coward, H. F. & Brinsley, F. 1914 *J. Chem. Soc.* **105**, 1859.
 Coward, H. F. & Jones, G. W. 1926 *Ind. Engng. Chem.* **18**, 970.
 Coward, H. F. & Jones, G. W. 1938 *U.S. Bur. Mines Bull.* 279 (revised).
 Dufraisse, C., Vieillefosse, R. & Le Braz, J. 1933 *C.R. Acad. Sci., Paris*, **197**, 162.
 Egerton, A. C. & Powling, J. 1948 *Proc. Roy. Soc. A*, **193**, 172, 190.
 Goldmann, F. 1929 *Z. Phys. Chem.* **5**, B, 307.
 Heilbron, I. M. 1934 *Dictionary of organic compounds*. London: Eyre & Spottiswoode.
 Jones, G. W. 1928 *Ind. Engng. Chem.* **20**, 367.
 Jones, G. W. 1929 *U.S. Bur. Mines Tech. Pap.* no. 450.
 Jones, G. W. & Perrott, G. St J. 1930 *U.S. Bur. Mines Rept. Invest.* 3042.
 Jones, G. W. & Scott, F. E. 1946 *U.S. Bur. Mines, Rept. Invest.* 3908.
 Olsen, J. C. & Graddis, A. H. 1938 *Ind. Engng. Chem.* **30**, 308.

Decay of isotropic turbulence in the initial period

By G. K. BATCHELOR, *Trinity College, University of Cambridge*
 AND A. A. TOWNSEND, *Emmanuel College, University of Cambridge*

(Communicated by Sir Geoffrey Taylor, F.R.S.—Received 4 December 1947)

In a previous paper the authors described direct measurements of all the terms in the equation for the rate of change of mean square vorticity in isotropic turbulence. The present paper is concerned with developments arising from the earlier work and with the experimental verification of some recent theoretical investigations. The results of measurements of the turbulent intensity u' and of λ are presented; these establish that u'^{-2} and λ^2 are each proportional to the time of decay provided that the time is not too large. Within this initial period of the decay, the double and triple velocity correlation functions are found to maintain their form, i.e. to be self-preserving, for small values of the distance r between the two points at which the correlations are taken. For larger separations the double velocity correlation function changes its form slightly during decay and direct measurements of λ and of the integral scale L show that λ/L increases during the decay. Theoretical predictions about the shape of the correlation function, for limited ranges of r , at high and at low Reynolds numbers are compared with measurements.

Theory has shown that the above decay law cannot persist indefinitely, and the present experiments confirm that the decay law changes in the expected direction when the time is large. A division of the life-history of the turbulence into initial, transition and final periods is suggested; within the initial period, a classification based on the Reynolds number is also possible. Some speculations on the interpretation of the initial period are presented.

1. INTRODUCTION

In a previous paper (Batchelor & Townsend 1947—referred to hereafter as I) the authors have analyzed measurements of the rate of change of mean square vorticity in isotropic turbulence. It has been shown theoretically that two separate physical processes contribute to the change in the vorticity. The first process is an average extension of the vortex lines due to the random diffusive motion, giving a positive contribution to $d\omega'^2/dt$, where ω'^2 is the mean square of any vorticity component, which is directly related to the skewness of the probability distribution of the rate of extension of fluid elements aligned in any direction. The second process is a dissipation of the vorticity due to the effect of viscosity, and the contribution to $d\omega'^2/dt$ depends on the fourth derivative at the origin of the double velocity correlation function. Both of these contributions and the value of $d\omega'^2/dt$ itself were measured at different stages in the decay of the turbulence. The agreement made it clear that it is permissible to apply the theory of isotropic turbulence to the motion behind a grid in a uniform stream and that the measurements described were essentially correct.

The plan of measuring all terms in an equation derived from the property of isotropy was also adopted for the energy balance. This equation contains only the mean energy per unit mass, $\frac{3}{2}u'^2$, and the dissipation length parameter λ , in addition to the independent variable t representing time. u'^{-2} and λ^2 were found to increase linearly with t , so that the Reynolds number $R_\lambda = u'\lambda/\nu$, was approximately constant for the range of grid Reynolds numbers and decay times used in the experiments. Once again the measurements were found to satisfy the equation.

Another result which emerged from the experiments was that there is some measure of self-preservation of shape of the functions $f(r)$ and $k(r)$ which describe the double and triple velocity correlations. f and k were found to be functions of the variable r/λ alone, not depending directly on t , so far as terms up to the fourth and third degree respectively in their expansions in powers of r are concerned. This property of self-preservation of the correlation functions is intimately related to the law of energy decay. One of us has therefore made a full theoretical analysis (Batchelor 1948—to be referred to as II) of the consequences of various kinds of self-preservation hypotheses under different Reynolds number conditions, and it has been found possible to make a number of predictions.

The present paper is in a direct sequence with the work of I and II. Its first aim is to determine the validity of the energy decay law reported in I over as wide a range of grid Reynolds numbers and decay times as the wind tunnel in the Cavendish Laboratory permits. The second aim is to examine the double velocity correlation at different decay times in order to see the extent of the property of self-preservation of shape. Finally, as many of the theoretical deductions of II as come within the scope of the measurements will be put to the test.

The measurements of the various statistical quantities associated with the turbulence have been made wholly with a hot-wire anemometer and wherever possible,

direct measurements obtained by a suitable electrical analysis of the wire output have been preferred. In this way direct measurements of u' , λ , $k_0''' \lambda^3$ and $f_0^{iv} \lambda^4$ as described in I, and of $\int_0^\infty f dr$, $g(r)$ and $k(r)$ have been made. Details of the methods are described fully in a separate paper by one of us (Townsend 1947). The wind tunnel used in the experiments is situated in the Cavendish Laboratory, Cambridge, and has been described in I. As is customary, the time of decay in the idealized problem of homogeneous isotropic turbulence will be identified with the time x/U which has elapsed since any point distance x from the turbulence-producing grid and moving with the mean stream was at the grid.

2. NOTATION TO BE USED

u'^2 = mean square fluctuation of any velocity component.

$\omega'^2 = 5u'^2/\lambda^2$ = mean square fluctuation of any vorticity component.

x = distance from the grid.

M = periodic spacing of the turbulence-producing grid.

d = diameter of the rods comprising the grid.

U = velocity of the uniform stream relative to the grid.

$R_M = UM/\nu$: Reynolds number associated with the grid.

$f(r)$, $g(r)$, $k(r)$: double and triple velocity correlation coefficients in the sense used in I and first defined by v. Kármán & Howarth (1938).

$$\lambda^{-2} = -\left(\frac{\partial^2 f}{\partial r^2}\right)_{r=0} = -\frac{1}{2}\left(\frac{\partial^2 g}{\partial r^2}\right)_{r=0}.$$

$$\psi = r/\lambda.$$

$R_\lambda = u'\lambda/\nu$: Reynolds number of the turbulence.

$L = \int_0^\infty f dr = 2 \int_0^\infty g dr$: integral scale of the turbulence.

$s = -k_0''' \lambda^3 = -\left(\frac{\partial u}{\partial x}\right)^3 \left[\left(\frac{\partial u}{\partial x}\right)^2\right]^{-1}$: skewness (with sign reversed) of the probability distribution of the rate of extension in any direction.

l = maximum value of r for which self-preservation of f , g and k occurs during the initial period.

C_D = drag coefficient of grid.

3. THE SIGNIFICANCE OF THE 'INITIAL PERIOD OF DECAY'

As a result of the experiments described in I and the theoretical analysis in II, it has become clear that there are two distinct phases in the life-history of isotropic turbulence produced by a grid, with a transitional phase connecting them. The phase which may be termed the *initial period of decay* is characterized by the existence of the energy decay law

$$u'^{-2} \propto t, \quad \lambda^2 = 10\nu t. \quad (3.1)$$

The measurements reported in I were made behind several grids ($M = 1.27, 2.54$ and 5.08 cm.) over ranges which lay within the limits $x/M = 20$ to $x/M = 130$ and the turbulence was in every case evidently within the initial period of decay. The range $x/M < 20$ is of course excluded from the system of classification since the turbulence takes a little time to become uniform (in the lateral direction) and isotropic. It remains to be seen whether it is possible to define an initial period of decay by the laws (3.1) for all values of the grid Reynolds number. The experiments of I covered the range $R_M = 5.5 \times 10^3$ to 4.4×10^4 and experiments to be described herein confirm the validity of the laws (3.1) in the initial period of decay for values of R_M at least down to 600.

Now in II it was shown theoretically that the only possible regime at very large times of decay is one in which the correlation functions are completely self-preserving and the law of energy decay is $u'^{-2} \propto t^{\frac{1}{2}}, \lambda^2 = 4\nu t$. (3.2)

The double velocity correlation function has the form

$$f(r) = e^{-r^2/2\lambda^2} \quad (3.3)$$

and the effect of the triple correlation is negligible. The authors propose that this phase be termed the *final period of decay*. There will also be a *transitional period of decay* when the mechanics of the turbulent motion is changing in type. As yet there is no definite information about the magnitudes of the decay times defining the extent of the different phases, but the experiments described below and others previously reported fix upper limits to the initial period for a few values of R_M .

It is possible to make, for the initial period of this fundamental division of the life-history of the turbulence into three phases, an equally fundamental classification depending on the magnitude of the Reynolds number. The basis for the classification lies in the relative effects on the turbulence of the inertia and viscous terms of the Navier-Stokes equations and a convenient analytical criterion can be obtained from the equation for decay of mean square vorticity. It was seen in I that this equation can be written as

$$\frac{3\sqrt{5}}{14} \frac{d\omega'^2}{dt} = \frac{s}{2} \omega'^3 - \frac{f_0^{iv} \lambda^4}{R_\lambda} \omega'^3. \quad (3.4)$$

Using the decay law (3.1) appropriate to the initial period, the left side becomes $-\frac{30}{7} \frac{\omega'^3}{R_\lambda}$, and the equation reduces to

$$\omega'^3 \left(-\frac{30}{7} \frac{1}{R_\lambda} = \frac{s}{2} - \frac{f_0^{iv} \lambda^4}{R_\lambda} \right). \quad (3.5)$$

The first term on the right side is derived from the inertia terms of the Navier-Stokes equations and represents the creation of mean square vorticity due to the diffusive increase in length of vortex lines. The second term on the right side represents the destruction of vorticity due to viscosity. Thus, the ratio of the viscous to the inertia effect is

$$\frac{2 f_0^{iv} \lambda^4}{s R_\lambda} = 1 + \frac{60}{7s} \frac{1}{R_\lambda}. \quad (3.6)$$

The experiments of I established for the initial period of decay and

$$0.5 \times 10^4 < R_M < 4.5 \times 10^4$$

that the skewness factor s is approximately an absolute constant with a value close to 0.39. Hence the factor which governs the relative importance of the viscous and inertia effects on the rate of change of mean square vorticity is

$$1 + \frac{22}{R_\lambda}. \quad (3.7)$$

The number R_λ clearly plays a fundamental role in the theory of isotropic turbulence and the authors propose to call it the Reynolds number of the turbulence. Since R_λ is constant during the initial period of the decay, the value of R_λ is a convenient and significant index to the type of turbulence occurring throughout that period. Three roughly separate regimes depending on the magnitude of R_λ can be distinguished. The regime of large Reynolds numbers of turbulence is such that $22/R_\lambda \ll 1$ and the contributions to $d\omega'^2/dt$ from the viscous and inertia terms are approximately equal and opposite. At intermediate Reynolds numbers the factor $22/R_\lambda$ is of order unity and the ratio of the two contributions to $d\omega'^2/dt$ is significantly different from unity. Finally, at small Reynolds numbers of turbulence, $22/R_\lambda \gg 1$, and the effect of the triple correlations on $d\omega'^2/dt$ is negligible compared with the viscous dissipation.

Each of these three regimes has its own body of theory. The existence of large Reynolds numbers of turbulence is basic to the theory of locally isotropic turbulence, first put forward by Kolmogoroff (1941) and developed more recently by one of us (Batchelor 1947). There is no need to describe here the results of this theory except to remark that it predicts that the skewness factor s is an absolute constant, and the experimental evidence (see I) for this result in the range of intermediate Reynolds numbers thus shows that there is some overlapping of the Reynolds number categories. There are other results of the theory, e.g. concerning the form of the function $f(r)$, which do not appear to be true at intermediate Reynolds numbers. There is as yet insufficient evidence to be certain that the energy decay law (3.1), which has been taken to define the initial period of decay, continues to hold as R_λ becomes large (the measurements described below confirm it as far as $R_\lambda = 60$), nor is this decay law necessary to the theory of locally isotropic turbulence, so that this part of the classification is provisional.

No unqualified deductions about the turbulence at intermediate Reynolds numbers have been made, but a few results have been obtained in II on the assumption of limited self-preservation of the correlation functions, i.e. that f and k are functions of r/λ only, provided $0 \leq r < l$, where l is an unspecified length which is not too large. There were found to be two possible ways of proceeding from this assumption. According to the first method of solution the law of energy decay is given by (3.1), whereas the second method gives a different decay law which asymptotes to (3.1)

at t increases. Since there is no means of predicting the rate of approach to (3.1), measurement of the energy decay law is not sufficient to choose between the two solutions. However they make different predictions about the correlation functions and the evidence presented below is sufficient to show that one solution is correct. When R_λ is small, it has been found possible (see II) to predict the form of the function $f(r)$ for as large a range of r as $f(r)$ is self-preserving during decay.

The experiments reported in I and those to be described below are concerned largely with the initial period of decay and with intermediate Reynolds numbers of turbulence. For three values of R_M the measurements have been made over a decay range which is sufficiently large to extend beyond the initial period and into the transitional period. Some results have been obtained under the conditions of large and small Reynolds numbers of turbulence and these show quite good agreement with the appropriate theoretical deductions.

4. RÉSUMÉ OF THEORETICAL RESULTS TO BE EXAMINED

The deductions which will be compared with experiment are set out in the following table. Reference should be made to the papers quoted for other deductions, from the same hypotheses, which do not lie within the scope of the experiments.

conditions	hypothesis	deductions
<i>initial period of decay</i>		
$\frac{22}{R_\lambda} \ll 1$	Kolmogoroff's similarity hypotheses	(a) $g(r) = 1 - \frac{2}{3}C \left(\frac{15}{R_\lambda} r \right)^{\frac{2}{3}}$, for $r \ll L$, where C is an absolute constant (b) $k_0'' \lambda^3$ and $f_0'' \lambda^4$ are constant if R_λ is constant during decay (c) s is an absolute constant } see I for verification
$\frac{22}{R_\lambda} = O(1)$	$f(r) \equiv f(r/\lambda)$, $k(r) \equiv k(r/\lambda)$, for $0 \leq r < l$	either (a) $R_\lambda = \text{constant}$ during decay, and $f'' + f' \left(\frac{4}{\psi} + \frac{5\psi'}{2} \right) + 5f + \frac{1}{2}R_\lambda \left(k' + \frac{4}{\psi} k \right) = 0$, for $0 \leq r < l$ (dashes denote differentiation with respect to ψ), or (b) an energy decay law which asymptotes to $R_\lambda = \text{constant}$, and $f'' + \frac{4}{\psi} f' + \left(\frac{5}{2} + \frac{7}{12}sR_\lambda \right) \psi f' + 5f = 0$, $k' + \frac{4}{\psi} k = \frac{7}{6}s\psi f'$, } for $0 \leq r < l$
$\frac{22}{R_\lambda} \gg 1$	$f(r) \equiv f(r/\lambda)$, for $0 \leq r < l$	$R_\lambda = \text{constant}$, and $f'' + f' \left(\frac{4}{\psi} + \frac{5\psi'}{2} \right) + 5f = 0$, for $0 \leq r < l$
<i>final period of decay</i>		
—	—	$u'^{-2} \propto t^{\frac{1}{2}}$, $\lambda^2 = 4\nu t$ and $f(r) = e^{-r^2/2\lambda^2}$

Downloaded from https://royalsocietypublishing.org/ on 04 August 2022

5. MEASUREMENTS OF u' AND λ

Measurements of the quantities u' and λ which occur in the energy equation, viz.

$$\frac{du'^2}{dt} = -\frac{10\nu u'^2}{\lambda^2}, \tag{5.1}$$

were made at various distances from a turbulence-producing grid. Four similarly shaped biplane grids constructed of circular cylinders of diameter $3M/16$ were used; the values of M were 5.08, 2.54, 1.27 and 0.635 cm. Measurements of λ were corrected for finite wire-length. The data are presented in figures 1 to 4. These diagrams contain the results described in I, together with new results for the smallest grid, and for the larger grids at different wind speeds. They summarize all the authors' experiments concerning the decay law (3.1), which is regarded as a characteristic of the initial period of decay.

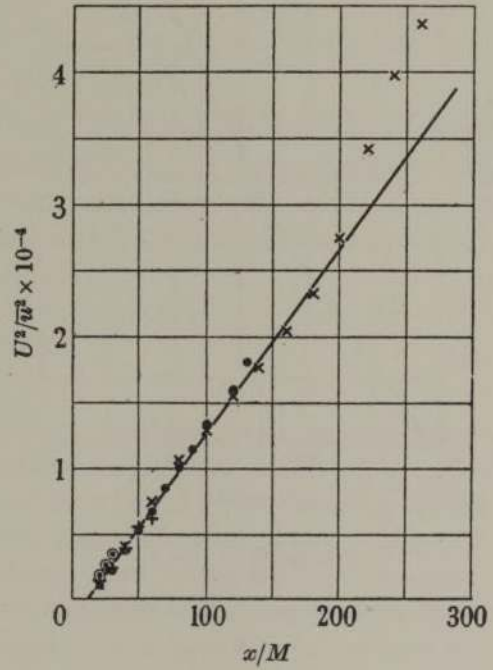
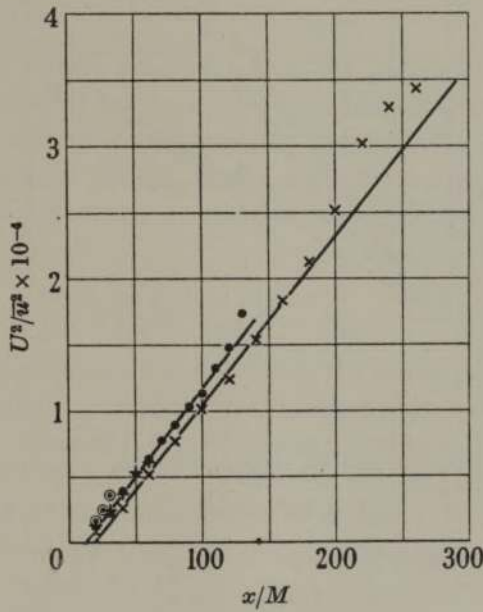


FIGURE 1. $\frac{u'^2}{U^2}$ vs. $\frac{x}{M}$ ($U = 643$ cm.sec.⁻¹).

FIGURE 2. $\frac{u'^2}{U^2}$ vs. $\frac{x}{M}$ ($U = 1286$ cm.sec.⁻¹).

\times $M = 0.635$ cm. \bullet $M = 1.27$ cm. $+$ $M = 2.54$ cm. \circ $M = 5.08$ cm.

It will be seen from figures 1, 2 and 3 that most of the measurements of U^2/u'^2 lie about a linear variation with x/M ; only at the large values of x/M obtained with the smallest mesh ($M = 0.625$ cm.) do the points depart appreciably from a straight line. It is thus possible to write

$$\frac{U^2}{u'^2} = \alpha \left(\frac{x}{M} - \frac{x_0}{M} \right) \tag{5.2}$$

Downloaded from https://royalsocietypublishing.org/ on 04 August 2022

for an initial range of values of x/M , where α and x_0 are constants. The energy equation (5.1) then requires

$$\lambda^2 = \frac{10\nu}{U} (x - x_0) = \frac{10M^2}{R_M} \left(\frac{x}{M} - \frac{x_0}{M} \right); \quad (5.3)$$

the rather curious but well-known result that λ^2 depends only on the viscosity and time of decay—depending not at all on M or U directly—is a consequence of any decay law which makes u'^2 vary as some power of x or t . In the plot of λ^2 vs. x in figure 4, lines are drawn with slope $10\nu/U$ and they represent well the experimental

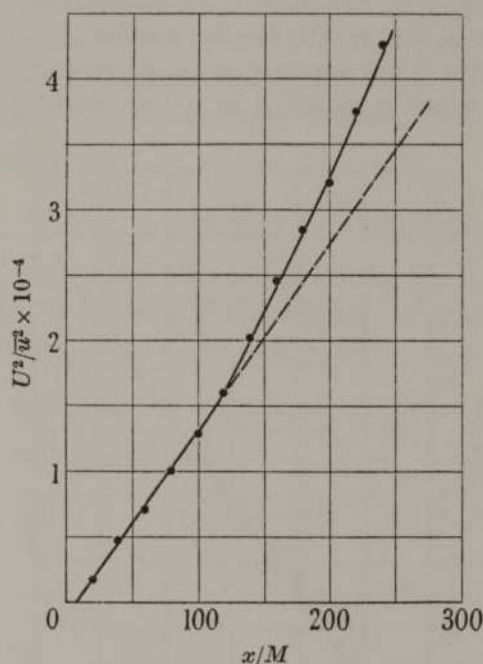


FIGURE 3. $\frac{u'^2}{U^2}$ vs. $\frac{x}{M}$

($U = 150$ cm.sec.⁻¹, $M = 0.635$ cm.)

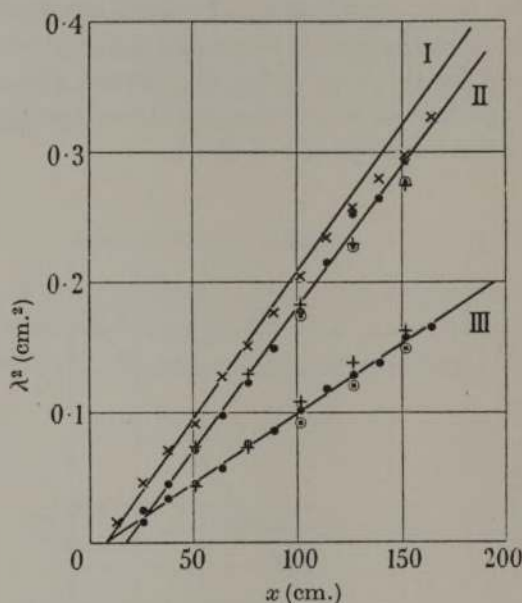


FIGURE 4. λ^2 vs. x

Curves I and II, slope = 2.26 cm. = $\frac{10\nu}{U}$
($U = 643$ cm.sec.⁻¹).

Curve III, slope = 1.13 cm. = $\frac{10\nu}{U}$
($U = 1286$ cm.sec.⁻¹).

× $M = 0.635$ cm. ● $M = 1.27$ cm.
+ $M = 2.54$ cm. ○ $M = 5.08$ cm.

variation, with the exception of the range $x/M > 180$ obtained with the smallest mesh. The experimental points would in no case be represented better by a straight line of slope more than 10% different from $10\nu/U$. Thus the power of $(x - x_0)$ which represents the variation of u'^{-2} in these experiments does not differ from unity by more than 10%.

The energy equation also requires the extrapolations of U^2/u'^2 and λ^2 to vanish at the same value of x . This virtual origin at $x = x_0$ represents the position at which

the turbulence is effectively created with infinite energy. Values of x_0 given by the straight lines best fitting observations of U^2/u'^2 and λ^2 (in the case of λ^2 the slope of the lines was taken as $10\nu/U$ and only the position was varied to improve the fit) are set out in table 1 and are approximately in accord.

TABLE 1. MEASUREMENTS OF u' AND λ BEHIND SIMILAR GRIDS

M (cm.)	U (cm.sec. ⁻¹)	R_M	$\left(\frac{x}{M}\right)_{U/u'=0}$	$\left(\frac{x}{M}\right)_{\lambda=0}$	$\frac{d(U^2/u'^2)}{d(x/M)}$	R_λ
0.635	643	0.28×10^4	20	12	128	14.4
1.27	643	0.55	12	13	132	20.3
2.54	643	1.10	10	7	130	28.7
5.08	643	2.21	3	5	—	41
0.635	1286	0.55	9	—	140	20.3
1.27	1286	1.10	15	5	151	28.7
2.54	1286	2.21	8	3	126	41
5.08	1286	4.42	6	3	—	58

Many investigators in the past have found that U^2/u'^2 when plotted as a function of x/M appears to be approximately independent of U and M for similar grids. The present measurements support this conclusion. Apart from the small change in virtual origin of the turbulence with R_M , there is a little variation (apparently random) in the slope factor α as shown in table 1.

$$\text{From (5.2) and (5.3)} \quad R_\lambda = \frac{u'\lambda}{\nu} = \left(\frac{10R_M}{\alpha}\right)^{\frac{1}{2}}, \quad (5.4)$$

and R_λ is constant during the initial period of decay. Knowledge of α for the types of grids commonly used in experiments therefore enables R_λ to be calculated for given values of U and M and as has already been seen, the value of R_λ is a significant index to the state of the turbulence. The data in table 1 show that the average value of α for the various values of M and U is 134 (no slope factor is deduced from measurements with $M = 5.08$ cm. since these could only be made over a very small range of values of x/M); this figure is appropriate to biplane grids for which the ratio of rod spacing M to diameter d is $\frac{1.6}{3}$. The values of R_λ calculated from (5.4) with $\alpha = 134$ are shown in the last column of table 1. They represent well the values of $u'\lambda/\nu$ obtained from the measurements of u' and λ except for the smallest values of x/M where the influence of the disparities in the virtual origins appropriate to the U^2/u'^2 and λ^2 curves is strong.

Measurements behind the grid of smallest M extended beyond the range of validity of the decay law (5.2). For $x/M > 180$ the measured values of U^2/u'^2 and λ^2 at all speeds show a rate of energy decay which is more rapid than that which holds in the initial period. The extent of the initial period of decay will probably depend on the grid Reynolds number and on the initial correlation functions created by the grid, but the tunnel available to the authors is too short to allow any systematic results

to be established. There appears to be a slow diminution in the extent of the initial period as R_M increases (see table 2 below).

Dryden (1943) has discussed the measurements of u' published by several authors and has compared them with the decay law (5.2). He finds moderately good agreement in all cases, particularly at the smaller values of x/M . In some cases the deviations found by Dryden can be interpreted as the beginning of the transitional period of decay. This is almost certainly true of v. Kármán's data. Von Kármán (1938) has presented measurements of u' behind four grids of the woven wire type with different values of M/d which, when plotted in the appropriate manner, show that U^2/u'^2 is initially proportional to x/M , but in some cases increases more rapidly for larger values of x/M . The essential features of v. Kármán's data are set out in table 2 for comparison with the measurements given by the authors. The point at which the linear decay law ceases to be valid is necessarily rather indefinite and the estimates given in the table are only useful as a guide.

TABLE 2. GRIDS OF DIFFERENT SHAPE

source	M (cm.)	M/d	UM/ν	upper limit to extent of initial period	$\frac{d(U^2/u'^2)}{d(x/d)}$ in initial period	$C_D \left[\frac{d(U^2/u'^2)}{d(x/M)} \right]$
v. Kármán	1.27	2.16	1.00×10^4	$x/M > 210$	7.0	128
v. Kármán	1.27	4.76	1.41	$x/M = 229 (?)$	3.1	106
v. Kármán	1.27	4.76	1.00	137	20.8	96
v. Kármán	1.27	6.04	2.00	113	23.6	90
v. Kármán	1.27	6.04	1.00	113	23.6	90
v. Kármán	1.27	11.6	2.00 1.00	no discernible initial period		
present authors	0.635	5.33	0.064	120	average for different M and U (see table 1) = 25.1	average for different M and U = 105
present authors	0.635	5.33	0.28	180		
present authors	0.635	5.33	0.56	200		

It has already been mentioned that the slope factor α of equation (5.2) appears to be independent of R_M for similar grids. It must thus be wholly determined by the characteristics of the grid which produces the turbulence. Two characteristics of the grid are relevant. The first is the drag per unit area, since it is the work done against this force which governs the amount of turbulent energy created by the grid. The second is the geometry of the grid, since this determines the length characteristics of the initial turbulence. These grid effects may be taken into account by writing

$$\frac{U^2}{u'^2} = \frac{\beta}{C_D} \left(\frac{x}{M'} - \frac{x_0}{M'} \right), \quad (5.5)$$

where β is an absolute constant, $C_D \cdot \frac{1}{2} \rho U^2$ is the drag of unit cross-sectional area of the grid and M' is an effective unit of length. M' will depend more on the spacing of the grid elements than on their dimensions.

Now when M/d is large, the drag of each grid element will be unaffected by the presence of its neighbours and C_D is proportional to d/M . This explains v. Kármán's observation that his measurements of U^2/u'^2 for the various grids came closer to coincidence when plotted against x/d rather than against x/M . However, table 2 shows there is still considerable variation in the value of $\frac{d(U^2/u'^2)}{d(x/d)}$ for the smaller values of M/d where the interference drag of the grid elements is appreciable. There have been many measurements of the drag of square grids of parallel circular cylinders in the past, and the formula which seems to represent the data best is*

$$C_D = \frac{\frac{d}{M} \left(2 - \frac{d}{M} \right)}{\left(1 - \frac{d}{M} \right)^4}. \quad (5.6)$$

Using this formula, the values of C_D for the grids used by v. Kármán and the present authors have been estimated and the last column of table 2 shows that the values of $C_D \left[\frac{d(U^2/u'^2)}{d(x/M)} \right]$ are more nearly constant than those of $\frac{d(U^2/u'^2)}{d(x/d)}$. The agreement is now as good as could be expected in view of the uncertainty of the estimates of C_D and of the difficulty in making absolute measurements of u' ; hence, so far as can be told from the data in table 2, the effective mesh length M' in (5.5) is approximately equal to M . β is given approximately by the average of the figures in the last column, with a total weight of unity for each group of readings which apply to one value of M/d , and (5.5) can be written approximately as

$$\frac{U^2}{u'^2} = \frac{106}{C_D} \left(\frac{x}{M} - \frac{x_0}{M} \right). \quad (5.7)$$

Further measurements are necessary before this relation can be applied with confidence to grids of arbitrary shape.

The formula (5.7) can also be written as

$$\frac{u_0'^2}{u'^2} = \frac{t}{t_0}, \quad (5.8)$$

which is more appropriate to the idealized problem of the decay of strictly homogeneous turbulence, since the factors related to the grid do not occur explicitly. $u_0'^2$ is the initial intensity of the turbulence created by the grid and is proportional to $C_D U^2$. t_0 is the time interval between the instant at which the extrapolated intensity would have been infinite and the initial instant at which it is $u_0'^2$. Evidently t_0 is proportional to M/U , as would be expected on the grounds that M and U are the factors most relevant to a time scale.

* See L. F. G. Simmons & C. F. Cowdray, Measurements of the aerodynamic forces acting on porous screens, *Aero. Res. Coun. Unpub. Rep.* 8920 (1945).

6. MEASUREMENTS OF $g(r)$ (a) *Limited self-preservation of $g(r)$*

The two double velocity correlation functions $f(r)$ and $g(r)$ are related by the continuity condition, viz.

$$g = f + \frac{r}{2} \frac{\partial f}{\partial r} \quad (6.1)$$

and a measurement of either is sufficient to determine the general double velocity correlation. Measurement of the lateral correlation is more convenient practically, and most of the $g(r)$ curve has been determined at a number of distances downstream from the grid for several values of U and M . Figures 5 to 8 exhibit the results. Each diagram refers to a single value of R_M and shows a family of curves of g against r/λ , each member of the family referring to a particular stage in the decay. The relative positions of the curves are sensitive to the values of λ at each value of x/M and so λ has been obtained from a smoothed experimental curve of λ against x/M . The method of measurement of g was less accurate at small values of r , but the parabolic variation of g near the origin has previously been verified and may be assumed with confidence.

Accurate self-preservation of the function g seems to hold for r/λ lying between 0 and some figure of the order of 1, the range being larger at the higher Reynolds numbers. A more satisfactory method of determining the extent of the self-preserving property is to measure directly the derivatives of $f(r)$ at $r = 0$ at different distances from the grid. Measurements of $f_0^{(v)} \lambda^4$, described in I, were found to be approximately constant during the decay. However, as mentioned in that paper, direct measurement of higher derivatives presents considerable difficulties.

The chief feature of each family is that, apart from within the self-preserving region, the values of r/λ corresponding to a given value of g decrease with increase of x/M . That is to say, outside the self-preserving region, the curves $g(\psi)$ of any family have roughly the same shape but contract laterally as x/M increases. Note however, that the change with x/M in the outer parts of the curves cannot be described exactly by such a contraction, for each curve must satisfy the identity

$$\int_0^\infty \psi g(\psi) d\psi = 0 \quad (6.2)$$

deduced from (6.1). The correlation functions f and g would be expected to diminish in absolute value at large values of r/λ with increase of x/M , since it was shown in II that

$$u'^2 \int_0^\infty f r^4 dr = \Lambda,$$

is constant during decay, and consequently, from (6.1),

$$\int_0^\infty \psi^4 f(\psi) d\psi = -\frac{2}{3} \int_0^\infty \psi^4 g(\psi) d\psi = \frac{\Lambda}{u'^2 \lambda^5}, \propto t^{-\frac{1}{2}}. \quad (6.3)$$

This relation is clearly consistent with a tendency for the curves of a family to contract slightly as t , or x/M , increases, since the absolute value of g diminishes with increase of r/λ when r/λ is large.

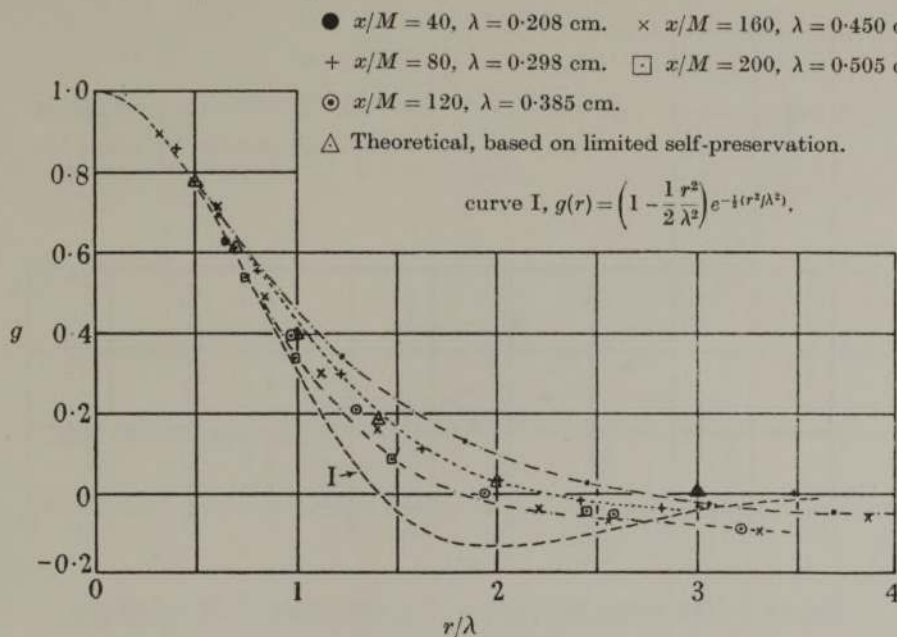


FIGURE 5. Transverse correlation. $U = 643$ cm.sec.⁻¹, $M = 0.635$ cm.,

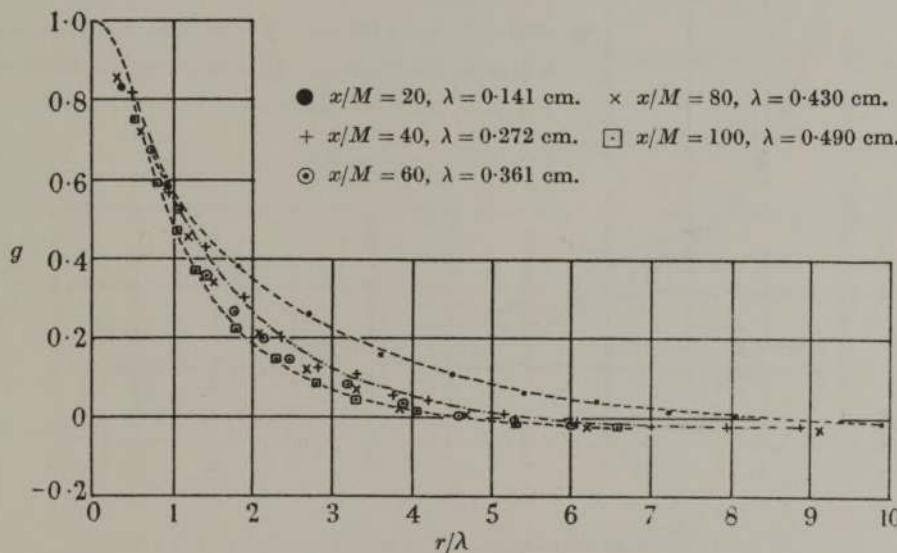


FIGURE 6. Transverse correlation. $U = 643$ cm.sec.⁻¹, $M = 1.27$ cm.

It follows from these considerations that the area $\int_0^\infty g(\psi) d\psi$ diminishes with x/M , and thence that the integral scale $L, = \int_0^\infty f dr = 2 \int_0^\infty g dr$, increases with x/M less rapidly than does λ . This is borne out by direct measurements of L , the

results of which are shown in figures 10 and 11. Figure 10 shows $(L/M)^2$ plotted against x/M and on the basis of similar evidence Dryden (1943) has represented the experimental variation by a straight line. At best this is an approximation, since

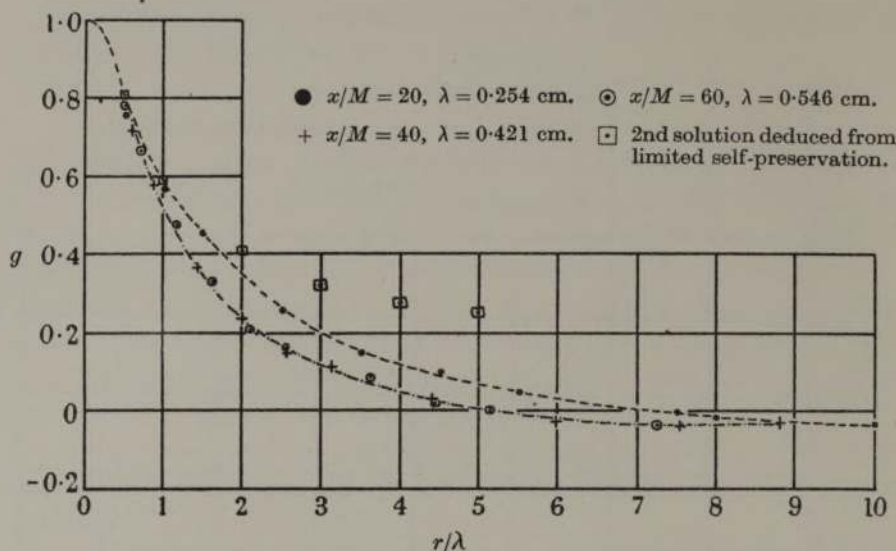


FIGURE 7. Transverse correlation. $U = 643$ cm.sec.⁻¹, $M = 2.54$ cm.

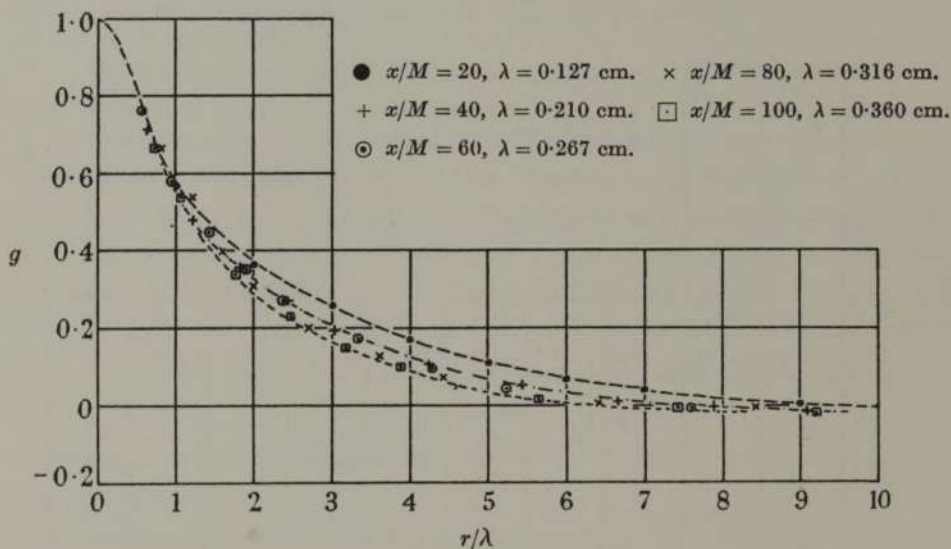


FIGURE 8. Transverse correlation. $U = 1286$ cm.sec.⁻¹, $M = 1.27$ cm.

an exact linear variation would imply complete self-preservation. It is doubtful whether the variation of L with x obeys any simple power law. Figure 11 shows that λ/L increases most rapidly when x/M is small, and is consistent with figures 5 to 8. The value of λ/L in the final period of decay is found from (3.3) to be $\sqrt{(2/\pi)} = 0.80$,

and this is presumably the asymptote toward which the curves of figure 11 ultimately tend. A point of interest about the measurements of scale is that at the virtual origin of the turbulence, L/M is in the neighbourhood of 0.3 or 0.4.

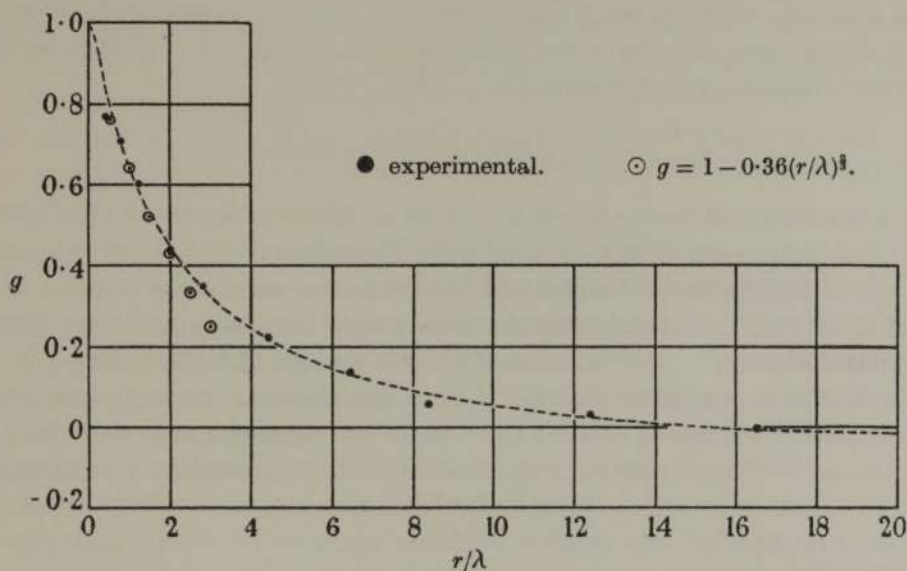


FIGURE 9. Transverse correlation. $U = 1286 \text{ cm. sec.}^{-1}$, $M = 5.08 \text{ cm.}$
 $x/M = 20$, $\lambda = 0.316 \text{ cm.}$

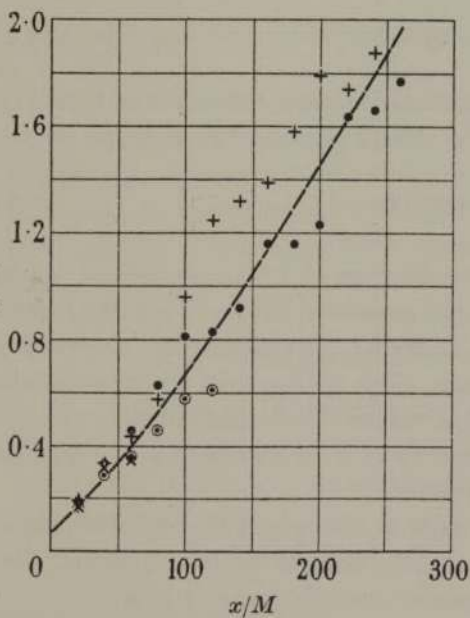


FIGURE 10. Variation of scale during decay.

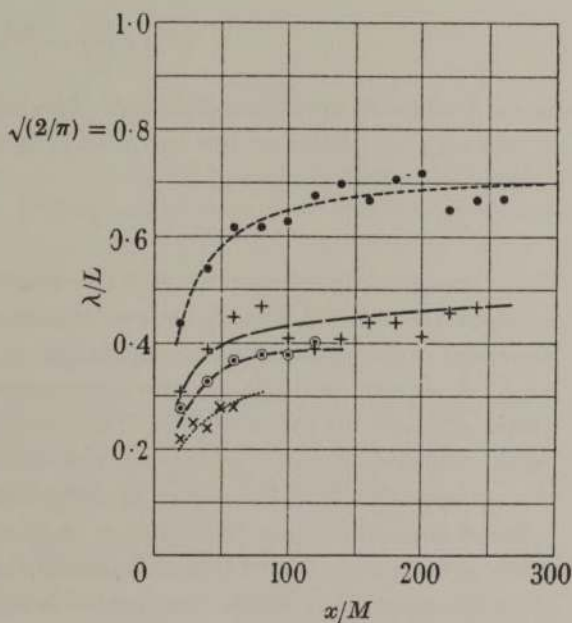


FIGURE 11. λ/L vs. x/M .

● $R_M = 2810$. + $R_M = 5620$. ○ $R_M = 11250$. × $R_M = 22500$.

(b) *Predictions about g*

It was stated in II that measurements of g would help to establish the validity of one of the two alternative deductions from the postulate of limited self-preservation. The first solution, which gives a decay law such that R_λ is constant, makes no prediction about f or g , but the second solution gives a decay law such that R_λ tends to a constant together with the equation

$$f'' + \frac{4}{\psi} f' + \left(\frac{5}{2} + \frac{7}{12}sR_\lambda\right) \psi f' + 5f = 0 \quad (r < l), \quad (6.4)$$

where s is the skewness factor found in I to be an absolute constant close to 0.39, and R_λ in (6.4) represents the asymptotic value. The solution of (6.4) can be obtained in the form of an indefinite integral and has been computed for a number of the values of R_λ at which measurements of g were made. Comparison of the measured and calculated curves of g as a function of ψ for one value of R_λ is shown in figure 7 and is typical of comparisons at other Reynolds numbers. The agreement is not good, particularly when it is recalled that one of the constants in the solution was chosen to make $f_0^{iv} \lambda^4$ agree with the value found by direct measurement (see I and II). Thus there is reason to reject the second of the two alternative deductions from limited self-preservation and further evidence given in §7 shows that the first solution is valid.

(c) *Solution for small values of R_λ*

A deduction from the postulate of limited self-preservation which is consistent with either of the solutions just mentioned is that, in the initial period of decay,

$$f'' + f' \left(\frac{4}{\psi} + \frac{5\psi'}{2} \right) + 5f = 0 \quad (6.5)$$

for $r < l$, when R_λ is sufficiently small. This equation describes the effect of viscosity on the smaller eddies of the turbulence in the initial period. The solution which makes $f = 1$ at $\psi = 0$ is

$$f(\psi) = \frac{3}{2} e^{-\frac{1}{2}\psi^2} \int_0^1 \tau^{\frac{1}{2}} e^{\frac{1}{2}\psi^2 \tau} d\tau. \quad (6.6)$$

The corresponding solution for $g(\psi)$ can be obtained from (6.1) and numerical values are shown in figure 5. This figure also contains the measured values of g at the lowest Reynolds number used in the correlation experiments. The agreement is good for $r/\lambda < 1.5$, except perhaps for the measurements close to the grid where accurate values of λ are difficult to obtain. The measured values of g become negative in the neighbourhood of $r/\lambda = 2$ whereas the solution (6.6) is everywhere positive; this sets an upper limit to the region of self-preservation.

Some departure from the solution (6.6) at $x/M = 200$ might be expected, since it has already been found that this position is slightly outside the initial period. The solution appropriate to the final period is obtained from (3.3) and (6.1) as

$$g = \left(1 - \frac{1}{2} \frac{r^2}{\lambda^2} \right) e^{-(r^2/2\lambda^2)} \quad (6.7)$$

and this curve is shown in figure 5 for comparison. The departures from the solution (6.6) at large values of x/M are in the direction to be expected from an approach to (6.7).

The value of R_λ for the measurements in figure 5 was 14.4, and the range of 'small' Reynolds numbers of turbulence such that the inertia forces play no part in the determination of the correlation function g (or f) therefore has its upper limit near this value. However, at this value of R_λ the ratio of the viscous to the inertia effect in the balance of mean square vorticity is only 2.5, so that the inner region of the correlation curve must be less sensitive to the effect of the inertia forces than the vorticity.

(d) *Large Reynolds numbers*

The present experiments were not designed to make possible a comparison of Kolmogoroff's theory of local isotropy with experiment, but the single measurement of the function g made at $R_M = 4.42 \times 10^4$ (see figure 9) may be used for this purpose. R_λ is here equal to 58 so that the ratio of the viscous to the inertia effect in the balance of vorticity is equal to 1.38. The theory predicts (Kolmogoroff 1941; Batchelor 1947) that

$$g(r) = 1 - \frac{3}{8}C \left(\frac{15r}{R_\lambda \lambda} \right)^{\frac{3}{2}} \quad (6.8)$$

provided $\eta \ll r \ll L$, where C is an absolute constant, η is a length of order $\lambda/\sqrt{R_\lambda}$ and L is the integral scale of turbulence. The curve of this shape which appears to fit the observations quite well is

$$g(r) = 1 - 0.36 \left(\frac{r}{\lambda} \right)^{\frac{3}{2}}.$$

The prediction (6.8) is thus successful if

$$C = 0.54 \left(\frac{R_\lambda}{15} \right)^{\frac{3}{2}} = 1.33,$$

which is quite close to the value 1.5 suggested by Kolmogoroff from a comparison with measurements made by Dryden. Other predictions from the theory of local isotropy (Batchelor 1947) have already been verified by the experiments described in I.

7. MEASUREMENT OF THE TRIPLE CORRELATION

It was shown in II that the two alternative deductions from the hypothesis of limited self-preservation lead to different predictions about the triple velocity correlation function k . According to the first solution, the decay law is such that R_λ is constant, and

$$f'' + f' \left(\frac{4}{\psi} + \frac{5\psi'}{2} \right) + 5f + \frac{1}{2}R_\lambda \left(k' + \frac{4}{\psi} k \right) = 0 \quad (7.1)$$

for $r < l$. Solving (7.1) for k ,

$$R_\lambda k(\psi) = -2(f' + \psi f) - \frac{3}{\psi^4} \int_0^\infty \psi^5 f' d\psi, \quad (7.2)$$

so that if f is measured, k can be calculated. On the other hand, the second solution leads to a decay law which makes R_λ tend to a constant value, and to the equations

$$f'' + \frac{4}{\psi} f' + \left(\frac{5}{2} + 0.23R_\lambda\right) \psi f' + 5f = 0, \quad (7.3)$$

$$k = \frac{0.46}{\psi^4} \int_0^\infty \psi^5 f' d\psi, \quad (7.4)$$

which can be solved to give both f and k in terms of R_λ . Both solutions give the correct value of k_0''' .

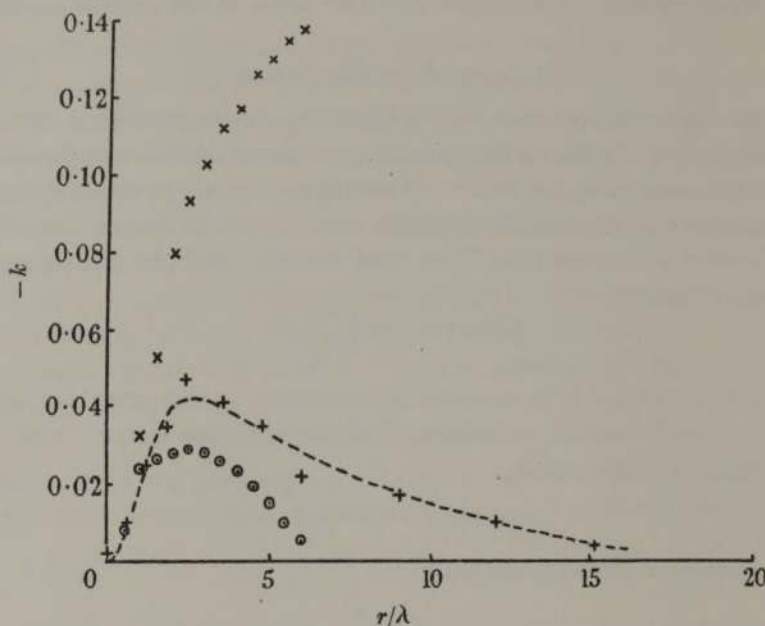


FIGURE 12. Triple correlation. + Experimental. \circ 1st solution; \times 2nd solution, both deduced from limited self-preservation.

A measurement of k for various values of r therefore provides a means of choosing between the two alternative deductions from the hypothesis of limited self-preservation. Figure 12 shows measurements of k at $x/M = 40$, for $M = 2.54$ cm., $U = 643$ cm.sec.⁻¹, and while no great accuracy is claimed for the measurements, they make it clear that the first solution is correct. The function k calculated from (7.2) and (6.1) by numerical integration of the values of g measured under the same conditions is shown in figure 12 and has the same shape as the measured curve for $r/\lambda < 4$. The ordinates of the calculated and measured curves differ in magnitude but this is probably due to the sensitivity of the integral in (7.2) to an error in the value of λ . Calculations of k from (7.3) and (7.4) with the appropriate value of R_λ are shown in figure 12 and do not give a curve of the correct shape. Hence, from the evidence of this and preceding section, it may be concluded that the initial period of decay is characterized by a decay law such that R_λ is constant and by the relation (7.1) between the double and triple correlations.

The measurements of k shown in figure 12 have considerable intrinsic interest, although the authors hope to be able to make more accurate determinations. When r is small, k is necessarily proportional to r^3 , and the curvature evidently decreases to zero rapidly as r increases. The maximum value of k is near $r/\lambda = 2.5$, and is followed by a slow fall to zero as r become large. The measurements of k are everywhere negative, which is the basis for an assumption that $\int_0^\infty k dr < 0$ used in II in the deduction that a completely self-preserving solution must occur when the time of decay is large.

8. INTERPRETATION OF THE INITIAL PERIOD

This paper would not be complete without some consideration of the physical processes occurring in the initial period of decay, although such considerations can be little more than speculation at the present time. The fundamental difficulty is to explain or deduce the law of energy decay found for this period. No acceptable deduction of this decay law—except that based on the assumption of limited self-preservation, which merely transfers the difficulty—has yet been put forward. Dimensional arguments have been used to deduce the energy decay law (Taylor 1935; Dryden 1943), but these assume that there is a single length characteristic of the turbulence and the experiments herein show this to be untrue. Such arguments can be successful if, and only if, they can show that the total amount of work done against Reynolds stresses created by the smaller scale velocity fluctuations is proportional to u'^3/λ . Since the dissipation of energy by viscosity is proportional to $\nu u'^2/\lambda^2$, consistency of the two expressions leads to $R_\lambda = \text{constant}$.

But once the decay law of the initial period is accepted, it is possible to understand—in the mathematical sense, at all events—why the period cannot continue indefinitely. For instance it was shown (see (6.3)) that

$$\int_0^\infty \psi^4 f(\psi) d\psi \propto t^{-1}$$

in the initial period. Near the origin, $f(\psi) \approx 1 - \frac{1}{2}\psi^2$ so that if f is to remain single-valued and positive, the above integral cannot decrease beyond a certain limit. Physically, the termination of the initial period seems to be a consequence of a continual narrowing of the range of sizes of eddies comprising the energy spectrum. At one end of the scale there is the length λ , which increases as \sqrt{t} . λ^{-2} is the mean square wave-number of sinusoidal velocity fluctuations, weighted according to their contribution to the total energy, so that λ is representative of the eddies of large wave-number, i.e. of the small eddies. At the other end of the scale is the integral scale L , representative of the largest eddies. L increases less rapidly than λ , so that the range is continually diminishing. A crisis develops, and whatever its nature, the net result is to reduce the rate of increase of λ .

The larger eddies lose their energy chiefly through the action of the inertia terms in the Navier-Stokes equations by transfer to smaller eddies, whereas the smaller

eddies are dissipated chiefly by the action of viscosity. At the end of a long period of decay, when the disparity in size between the largest and smallest eddies has been reduced appreciably and the Reynolds number of the larger eddies has diminished, viscosity becomes a significant factor in the reduction in energy of all the eddies. It is reasonable to expect a fundamental change in the decay law then to occur. During the transitional period the inertia terms continue to play some part in the transfer of energy away from the larger eddies, but the Reynolds number is decreasing with time, and in the final period of decay viscosity dominates the mechanics of the turbulence. The large negative value at the minimum of the correlation function g which holds in the final period (see equation (6.7) and figure 5) is an indication that the eddies existing in the final period are more uniform in type and size than in the initial period.

Thanks are due to Professor Sir Geoffrey Taylor for his stimulating interest in the work. During the course of the research the authors were in receipt of a Senior Studentship (G.K.B.) and an Overseas Scholarship (A.A.T.) from the Royal Commission for the Exhibition of 1851. Component parts of the measuring equipment were purchased with money provided by the Aeronautical Research Council.

REFERENCES

- Batchelor, G. K. 1947 *Proc. Camb. Phil. Soc.* **43**, 533-559.
 Batchelor, G. K. 1948 *Quart. App. Math.* **6** (referred to in the text as II).
 Batchelor, G. K. & Townsend, A. A. 1947 *Proc. Roy. Soc. A*, **190**, 534 (referred to as I).
 Dryden, H. L. 1943 *Quart. App. Math.* **1**, 7-42.
 Kármán, T. v. 1938 *Proc. 5th Int. Cong. App. Mech.* pp. 347-351.
 Kármán, T. v. & Howarth, L. 1938 *Proc. Roy. Soc. A*, **164**, 192-215.
 Kolmogoroff, A. N. 1941 *C.R. Acad. Sci. U.R.S.S.* **30**, 301-305 and **32**, 16-18.
 Taylor, G. I. 1935 *Proc. Roy. Soc. A*, **151**, Part I, 421-444.
 Townsend, A. A. 1947 *Proc. Camb. Phil. Soc.* **43**, 560-570.